Journal of Pharmaceutical Analysis 14 (2024) 100938

Contents lists available at ScienceDirect

Journal of Pharmaceutical Analysis

journal homepage: www.elsevier.com/locate/jpa

Short communication

Discovery of potent anti-MRSA components from *Dalbergia odorifera* through UPLC-Q-TOF-MS and targeting PBP2a protein through in-depth transcriptomic, *in vitro*, and *in-silico* studies

Jiajia Wu [a], Syed Shams ul Hassan [a], Xue Zhang [a], Tao Li [b, **], Abdur Rehman [c], Shikai Yan [a], Huizi Jin [a, *]

[a] Shanghai Key Laboratory for Molecular Engineering of Chiral Drugs, School of Pharmacy, Shanghai Jiao Tong University, Shanghai, 200240, China
[b] Shanghai Veterinary Research Institute, Chinese Academy of Agricultural Sciences, Shanghai, 200241, China
[c] College of Life Sciences, Northwest A&F University, Yangling, Shaanxi, 712100, China

ARTICLE INFO

Article history:
Received 9 September 2023
Received in revised form
7 January 2024
Accepted 17 January 2024
Available online 23 January 2024

Methicillin-resistant *Staphylococcus aureus* (MRSA) is an important pathogen casting dire shadow over global human well-being [1]. Rising antibiotic resistance in MRSA led to research into plant-derived anti-microbial agents. Approximately 119 compounds from 90 plants were recognized as potent anti-bacterials [2]. *Dalbergia odorifera*, a traditional Chinese plant, has demonstrated anti-tumor, anti-microbial, anti-inflammatory, and cardiovascular protective effects [3]. Limited studies have explored *D. odorifera* flavonoids' inhibitory activity against MRSA. Transcriptomics, a high-throughput method, aided in comprehending plant antibacterial therapy by generating data for gene expression, target identification, and pathway analysis [4]. Consequently, our study aimed to assess *D. odorifera*'s anti-MRSA effects and reveal its material foundation and antibacterial mechanism by ultra-performance liquid chromatography coupled with quadrupole time of flight mass spectrometry (UPLC-Q-TOF-MS), and transcriptomic analysis, *in vitro*, and *in-silico* studies.

Based on indigenous knowledge of *D. odorifera*, we obtained extracts of varying-polarity (petroleum ether (PE), ethyl acetate (EA), *n*-butanol (nBu)) from four organs (stem, leaf, flower, and heartwood) (Fig. S1). Detailed methods are provided in the Supplementary data. The comprehensive gas chromatography-mass spectrometry (GC-MS) analysis identified and quantified 28, 28, 22, and 24 components in the PE extract of leaf, stem, flower, and heartwood, respectively (Fig. S2). The leaf-PE was rich in hexadecenoic-acid ethyl ester (11.23%), hexamethyl-cyclotrisiloxane (11.20%), and octamethyl-cyclotetrasiloxane (7.76%) (Table S1, and Fig. S3A). Stem-PE contained hexadecenoic-acid ethyl ester (11.93%), octadecanoic-acid ethyl ester (6.79%), and 2,4-di-*tert*-butylphenol (6.42%) as major components (Table S2, and Fig. S3B). Flower-PE had hexamethyl-cyclotrisiloxane (10.22%), hexadecenoic-acid ethyl ester (9.07%), and dodecamethyl-cyclohexasiloxane (7.86%) as major constituents (Table S3, and Fig. S3C). However, distinct from other parts, medicarpin (11.69%) and nerolidol (3.16 %) were identified as distinctive compounds in heartwood-PE possessing diversified pharmacological effects (Table S4, and Fig. S3D). Venn analysis revealed overlap in volatile components among four parts, with 12 shared components. Conversely, heartwood exhibited distinctiveness with 19 unique-components (Fig. 1A). The Venn network (Fig. S4) highlighted two shared high-content components in four extracts, namely hexadecenoic-acid ethyl ester and linoleic-acid ethyl ester. Thus, the antimicrobial and anti-inflammatory properties of the low-polarity *D. odorifera* extract attributed to abundant lipid composition.

Rapid qualitative analysis of non-volatile components in EA and nBu extracts of *D. odorifera* were detected using UHPLC-Q-TOF-MS/MS (Fig. S5), and 31 and 33 components were identified in leaf-EA and leaf-nBu extract, respectively (Fig. 1B, and Tables S5 and S6). Concurrently, the flower-EA and flower-nBu extracts contained 36 and 46 chemical components, respectively (Fig. 1B, and Tables S7 and S8). Profiling non-volatile ingredients of leaf and flower unveiled 39 shared compounds, with only 3 compounds exclusive to leaf, while 17 unique compounds were found in flower (Fig. S6A). Remarkably, Fig. S6B strongly supported flavonoids as the primary constituents in the non-volatile ingredients of *D. odorifera*. Flavonoids in *D. odorifera* were well-established for their significant bioactivity [5].

Based on component characterization, *in vitro* anti-bacterial screening of different extract from four parts of *D. odorifera* was conducted (Table S9), and heartwood displayed significant broad-

* Corresponding author.
** Corresponding author.
E-mail addresses: litao@shvri.ac.cn (T. Li), kimhz@sjtu.edu.cn (H. Jin).

https://doi.org/10.1016/j.jpha.2024.01.006

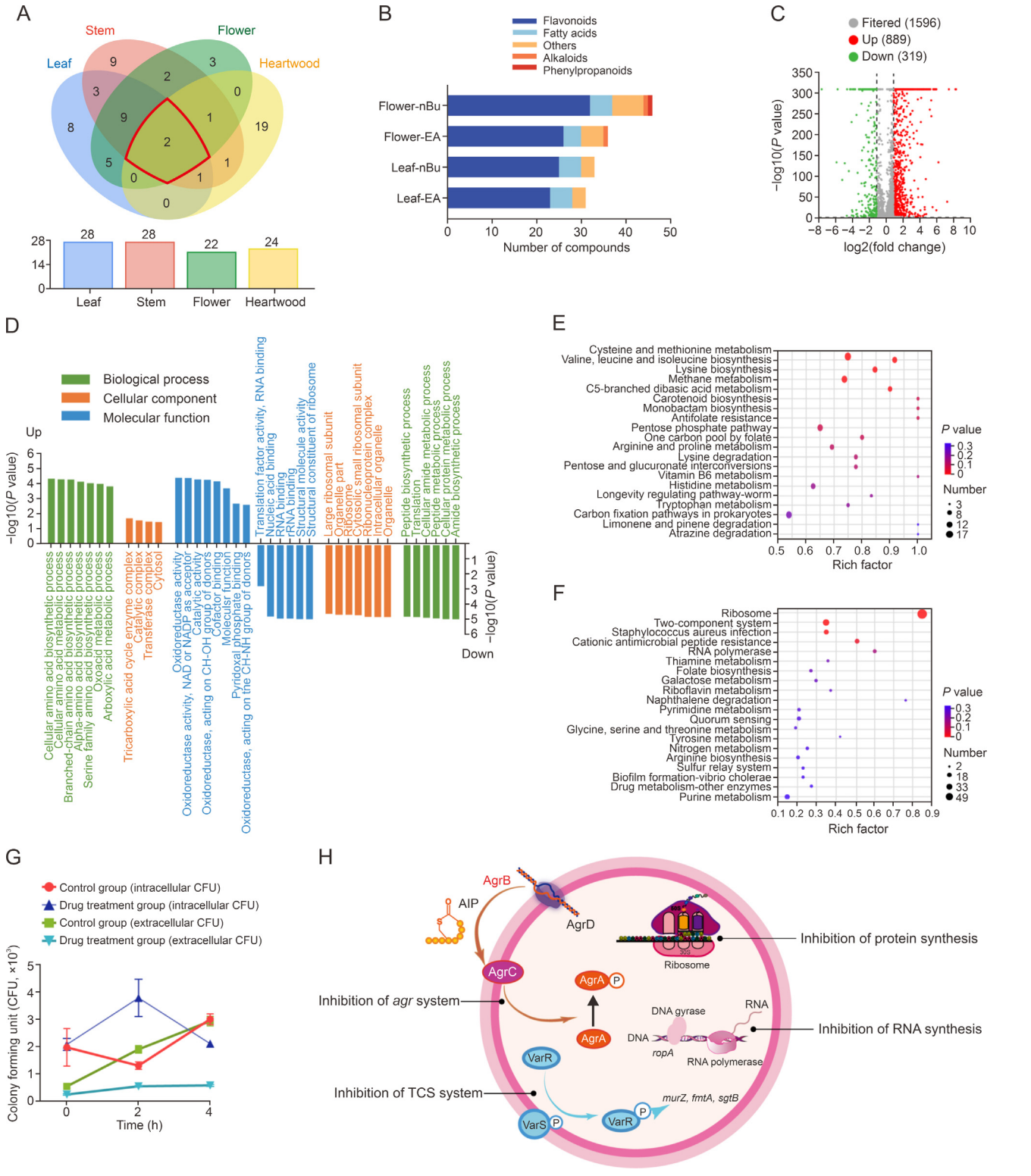

Fig. 1. Relationship between volatile and non-volatile components in different parts extracts in *D. odorifera*, and transcriptomic analysis of differentially expressed genes (DEGs) in heartwood-petroleum ether (PE) treated group. (A) Classical Venn diagram for volatile components in leaf, stem, flower, and heartwood extracts. (B) The number of non-volatile compounds identified in ethyl acetate (EA) and n-butanol (nBu) extracts of leaf and flower. (C) Volcano plot of DEGs. (D) Gene Ontology (GO) enrichment analysis of DEGs. (E) Kyoto Encyclopedia of Genes and Genomes (KEGG) enrichment analysis of up-regulated DEGs. (F) KEGG enrichment analysis of down-regulated DEGs. (G) The intracellular and extracellular distribution of *Methicillin*-resistant *Staphylococcus aureus* (MRSA) strains at different time intervals following drug treatment. (H) Proposed multi-target mechanisms for antibacterial activity of *D. odorifera* against MRSA, including inhibition of translation function of ribosome, decreased expression of *rpoA* and inhibition of RNA synthesis, decreased expression of *agrB* and disruption AGR-mediated toxin production, and decreased expression of *varRS*-regulated genes of *murZ*, *fmtA*, and *sgtB* and inhibition of cell wall synthesis.

spectrum anti-bacterial activity against all tested bacteria. Visual analysis of *Staphylococcus aureus* and MRSA (Fig. S7) revealed that heartwood possessed the highest anti-bacterial efficacy against strains, followed by flower and stem extracts. PE-extracts exhibited superior anti-bacterial potency compared to EA and nBu-extracts. Volatile component analysis identified medicarpin and nerolidol as representative components in heartwood-PE. Further tests showed that medicarpin inhibited *Staphylococcus aureus* and MRSA by 84.63% and 85.35%, respectively, while nerolidol displayed remarkable inhibition against *Staphylococcus aureus* (89.24%) and MRSA (67.28%).

Given these compelling results, we selected heartwood-PE for transcriptomic analysis, obtaining high-quality and reliable RNA samples from both the heartwood-PE treatment and control groups (Tables S10 and S11). A total of 1,208 differentially expressed genes (DEGs) were identified, comprising 889 upregulated and 319 downregulated DEGs (Fig. 1C). Gene Ontology (GO) analysis revealed DEGs associations with amino acid metabolism and biosynthesis in biological process, following heartwood-PE treatment (Fig. 1D). Concerning cellular components, DEGs were prominently enriched in ribosomal components. Molecular function analysis indicated marked upregulation of DEGs related to oxidoreductase and catalytic activities, whereas downregulated DEGs were associated with ribosomal structure, rRNA binding, and translation factors, suggesting disruptions in ribosome-related structural and function. Furthermore, Kyoto Encyclopedia of Genes and Genomes (KEGG) analysis revealed that under *D. odorifera* treatment, MRSA restricted exogenous amino acid uptake, reciprocally modulating genes associated with amino acid biosynthesis and metabolism. Specifically, upregulated pathways encompassed valine, leucine, lysine, and cysteine biosynthesis and metabolism (Fig. 1E). The most representative downregulated pathways were associated with ribosome pathways, nutrient transport, signal transduction, and substance metabolism (Fig. 1F).

Using an MRSA cellular infection model with HD11 cells, we assessed MRSA's intracellular and extracellular distribution at varying post-drug treatment time intervals (Fig. 1G). Compared to the control group, the heartwood-PE group initially showed increased MRSA intracellular colony-forming-units (CFU), followed by a decrease, while extracellular MRSA CFU steadily increased. Results suggested that during the initial phases of heartwood-PE treatment, MRSA temporarily entered cells to evade drug-induced bactericidal effects, diminishing bacterial eradication efficacy. This phenomenon highlighted the need for clinical vigilance against recurrent bacterial infections post-treatment.

In the study, DEGs analysis revealed key genes in amino-acid metabolism and protein synthesis. Genes, *cysNC*, *cysD*, *sirA*, and *subI*, exhibited enhanced expression, participating in amino acid biosynthesis (e.g., cysteine and methionine) (Table S12). This confirmed that *D. odorifera* treatment caused amino acid imbalance in MRSA, with the bacteria countering environmental stress by regulating amino acid synthesis. Conversely, genes encoding ribosomal proteins 30S and 50S (e.g., *rpsD*, *rplD*) showed significant downregulation (Table S13). Simultaneously, genes for translation initiation factor IF-3 (*infC*) and peptide release factor (*prfA*) displayed reduced-expression, indicating *D. odorifera*'s inhibitory effect on MRSA ribosomal translation and protein synthesis. We observed *rpoA* downregulation, impacting RNA polymerase function, revealing interference with RNA synthesis in *D. odorifera*'s antibacterial mechanis. Additionally, *D. odorifera* inhibited two-component systems (TCSs) and the accessory gene regulator (AGR) quorum sensing system. It targeted AGRs' upstream signaling pathway (downregulating *agrB* and *agrD*), inhibiting auto-inducing peptides (AIP) biosynthesis, disrupting AGR-mediated toxin production, and exerting antibacterial effects. Furthermore, *D. odorifera* increased sensitivity to cell wall synthesis inhibitors, downregulating *varR*, *sgtB*, *murZ*, and *fmtA* via TCS impairment, ultimately inhibiting MRSA cell wall formation (Fig. 1H).

Medicarpin and nerolidol displayed robust molecular docking interactions with MRSA's PBP2a and DNA gyrase A proteins, suggesting their potential as effective antibacterial agents (Table S14, and Fig. S8). Subsequent molecular simulations revealed that the medicarpin-PBP2a complex exhibited initial fluctuations within the first 10 ns, followed by stable binding after 17 ns, which persisted until the simulation's end (Fig. S9A). The medicarpin-DNA gyrase A complex remained highly stable throughout the entire trajectory, with minor fluctuations between 15 ns and 20 ns (Fig. S9B).

This study demonstrated the potential of *D. odorifera* heartwood-PE as MRSA bacteriostat. We characterized volatile and non-volatile components across medicinal parts, identifying 63 volatile and 59 non-volatile components. *In vitro* screening showed the heartwood-PE's strong anti-MRSA activity. Transcriptomic and bioinformatics analysis revealed *D. odorifera*'s impact on critical MRSA survival processes, including RNA synthesis, transcription, protein translation, and emerging targets like TCS and AGR system. MRSA adapted by enhancing specific amino acid synthesis. Medicarpin and nerolidol, major compounds in the heartwood-PE, exhibited strong binding to MRSA's PBP2a and DNA gyrase A proteins in molecular simulations.

While our study highlights *D. odorifera*'s potential as an effective MRSA antibacterial agent and elucidates molecular mechanism. Further molecular biology of pathway validation is needed to enhance the clinical application of *D. odorifera* as therapeutic agent for MRSA.

CRediT authorship contribution statement

Jiajia Wu: Data curation and Writing – original draft preparation; **Syed Shams ul Hassan:** Software and Writing – review & editing; **Xue Zhang:** Investigation and Methodology; **Abdur Rehman:** Software; **Shikai Yan:** Formal analysis; **Tao Li:** Validation and Supervision; **Huizi Jin:** Project administration and Funding acquisition.

Declaration of competing interest

The authors declare that there are no conflicts of interest.

Acknowledgments

We are extremely grateful to the National Natural Science Foundation of China (Grant No.: 81973191), Shanghai Agriculture Applied Technology Development Program, China (Program No.: T20200104), and the National Key Research and Development Program of China (Program No.: 2018YFE0192600) for providing financial support for the complete undertaking.

Appendix A. Supplementary data

Supplementary data to this article can be found online at https://doi.org/10.1016/j.jpha.2024.01.006.

References

[1] L. Sun, H.B. Zhang, H.H. Zhang, et al., Staphylococcal virulence factor HlgB targets the endoplasmic-reticulum-resident E3 ubiquitin ligase AMFR to promote pneumonia, Nat. Microbiol. 8 (2023) 107–120.

[2] S.N.A. Adnan, N. Ibrahim, W.A. Yaacob, Transcriptome analysis of methicillin-resistant *Staphylococcus aureus* in response to stigmasterol and lupeol, J. Glob. Antimicrob. Re. 8 (2017) 48–54.
[3] H.M. Yun, K.R. Park, T.H. Quang, et al., 2,4,5-Trimethoxyldalbergiquinol promotes osteoblastic differentiation and mineralization via the BMP and Wnt/β-catenin pathway, Cell Death Dis 6 (2015), e1819.
[4] X.J. Tian, Q.Q. Yu, L.L. Shao, et al., Comparative transcriptomic study of *Escherichia coli* O157:H7 in response to ohmic heating and conventional heating, Food Res. Int. 140 (2021), 109989.
[5] H. Meng, X.Y. Xia, G.X. Ma, et al., Chemical constituents and anti-inflammatory activity from heartwood of *Dalbergia odorifera*, Nat. Prod. Res. Dev. 30 (2018) 800–806.